2nd Faculty of Medicine
Charles University in Prague

Institute of Physiology
Academy of Sciences of the Czech Republic, vvi

A study on the effect of ivermectin at purinergic $P2X_4$ receptor

Irena Jelínková

Summary of PhD Thesis

Prague 2007

This PhD thesis was elaborated at the Department of Cellular and Molecular Neuroendocrinology and the Department of Protein Structure of the Institute of Physiology, Academy of Sciences of the Czech Republic, Prague. It is a completion of the PhD studies of Biomedicine at the 2nd Faculty of Medicine, Charles University in Prague, specialization Biochemistry and Pathobiochemistry.

Applicant:	Irena Jelinkova
Address:	Institute of Physiology, AS CR, vvi Videnska 1083 142 20 Prague 4 Czech Republic Phone: +420 29644 2737 Fax: +420 29644 2488 Email: jelinkoi@biomed.cas.cz

Commission:	Biochemistry and Pathobiochemistry
Supervisor:	Jan Teisinger, Ing., CSc.
Consultants:	Hana Zemkova, RNDr., CSc.
Opponents:	
Summary was sent out on:	
Defence of the thesis:	
Chairman of the Commission:	Prof. MUDr. J. Kraml, DrSc.

Table of Contents

1. Summary

P2X$_4$ receptor is ATP-gated cation channel. It is the only mammalian purinergic receptor which is modulated by extracellularly applied ivermectin (IVM). IVM has several effects on receptor function: it increases sensitivity to agonists, potentiates maximum current amplitude and prolongs the deactivation kinetics of the channel after agonist washout.

We focused on identification of regions and residues responsible for IVM effect on channel function. We used several chimeras of P2X$_2$/P2X$_4$ receptors and several single point mutants of P2X$_4$ receptor. Experiments with chimeric receptors revealed that extracellular sequence V49-V61 but not the sequence V64-Y315 is important for the effects of IVM on channel deactivation. Receptor-specific point alanine mutations placed in transmembrane domains G29-V61 and N338-L358 showed the potential importance of residues W50, V61 and V357 for IVM effect on channel deactivation. We tested further the importance of receptor-nonspecific residues in transmembrane domains. Cysteine scanning mutagenesis supported the relevance of previously identified W50 residue and showed the importance of residues G29, R33, Q36, L40, V43, V47, N338, G342, L346, A349 and I356 for the binding of the IVM molecule to the P2X$_4$ receptor.

We used IVM also as a pharmacological tool to evaluate the role of several ectodomain residues presumably involved in the ATP binding and/or channel gating mechanism. We created alanine and rescue mutations of K67, F185, K190, F230, R278, D280, F294, R295 and K313 residues. The majority of these mutant receptors were low-responsive or non-responsive to ATP; however, the modulatory effect of IVM was preserved. In the presence of IVM, we observed differences in ATP sensitivity and channel deactivation suggesting different role of mutated residues for channel function. The results of our experiments indicate that residues K67, R295 and K313 are critical for ATP binding or channel gating in P2X$_4$ receptor.

2. Introduction

Purinergic P2X receptors are a family of ligand gated nonselective cation channels, which are activated by extracellular ATP. A single P2X receptor subunit is composed of intracellular N- and C-termini, two transmembrane domains (TM1 and TM2) and large extracellular loop. There are seven mammalian P2X subunits, called $P2X_{1-7}$, which all share similar structure (Brake, Wagenbach et al. 1994; Valera, Hussy et al. 1994; Newbolt, Stoop et al. 1998; Torres, Egan et al. 1998). Functional channels are formed as homo- or heterotrimers (Nicke, Baumert et al. 1998; Barrera, Ormond et al. 2005). In the past ten years, the P2X receptors have been investigated intensively. However, only little is known about their function and structure.

P2X channels are permeable to small monovalent cations, Ca^{2+} or small organic cations (North 2002). The pore of the channel is formed by both TM domains but their organization is largely unknown. The TM domains are close to each other since the intersubunit disulfide bond have been observed between V48C and I328C in $P2X_2$ receptor (Jiang, Rassendren et al. 2001; Khakh and Egan 2005). It has been suggested that TM1 adopts α-helical structure while for the TM2 this secundary structure has not yet been proven (Rassendren, Buell et al. 1997; Egan, Haines et al. 1998; Li, Migita et al. 2004; Silberberg, Chang et al. 2005). The results of alanine scanning mutagenesis performed on $P2X_2$ receptor showed that TM1 residues F31, R33 and Q37 participate in channel dilatation (Khakh and Egan 2005) and residues in the upper half of TM1, especially Y43 and F44, affect channel sensitivity to agonists (Haines, Migita et al. 2001; Li, Migita et al. 2004). The TM2 residue G347 ($P2X_2$), which is on the boarder between the inner and outer part of the pore, has been suggested to be a joint that enables opening and closing of the pore (Egan, Haines et al. 1998; Li, Migita et al. 2004; Khakh and Egan 2005). The selectivity filter of the channel might be formed by participation of T336, T339 and S340 residues ($P2X_2$) (Migita, Haines et al. 2001).

The ATP binding site is located in the extracellular domain, but its structure has not yet been identified. Since the sensitivity of P2X receptors to ATP is

different the structure of ATP binding region is supposed not to be identical (Gever, Cockayne et al. 2006). It is assumed that one receptor molecule contains 3 ATP binding sites which are probably localized between subunits (Wilkinson, Jiang et al. 2006). Many proteins, which interact with ATP, coordinate the molecule of ATP by lysine, arginine or phenylalanine residues. These amino acids were tested also for P2X receptors and several models of ATP binding site have been proposed. Evans et al. created a model of $P2X_1$ receptor in which the adenine ring is coordinated by residues F185, T186, N290, F291 and R292. Positively charged residues K68 and K309 coordinate β- a γ-phosphate groups and R292 interact with α-phosphate (Ennion, Hagan et al. 2000; Roberts and Evans 2004; Vial, Roberts et al. 2004; Roberts and Evans 2006; Roberts, Vial et al. 2006). Other model was proposed by Freist et al. who found similarity between the sequence of aminoacyl-tRNA-synthetases (group II) and P2X receptor subunits (Freist, Verhey et al. 1998). This similarity was also used by Yan et al. for model of ATP binding site at $P2X_4$ receptor (Yan, Liang et al. 2005). In this model, residue D280 coordinates Mg^{2+} binding, F230 interacts with adenine ring, K190 interacts with α-phosphate and H286 and R278 coordinate β- and γ-phosphate groups, respectively. Residue R318 participates in transduction of the signal from ATP binding site to the gate. Also residue K313 plays an important role in channel function but not in ATP binding (Yan, Liang et al. 2005).

In this study we focused on $P2X_4$ receptor. This receptor is expressed in many mammalian organs including brain and is implicated in several physiological functions (Gever, Cockayne et al. 2006). It is characterized by fast internalization and slow recovery from desensitization. The $P2X_4$ receptor is unique among the mammalian P2X family for its ability to be positively modulated by ivermectin (IVM) (Khakh, Proctor et al. 1999), highly lipophilic compound used in human and veterinary medicine for the treatment of parasitic diseases (Edwards 2003). IVM acts on $P2X_4$ channels as an allosteric modulator. When applied extracellularly it increases amplitude of ATP-induced current, prolongs channel deactivation and increases the sensitivity to agonists (Khakh, Proctor et al. 1999; Priel and Silberberg 2004). The binding site for IVM at $P2X_4$ receptor has not yet been described.

The selectivity and positive modulatory effect makes IVM a useful pharmacological tool for investigation of $P2X_4$ channel function. In this work we focused on the identification of $P2X_4$ receptor-specific residues and regions contributing to IVM effects on this channel. Furthermore, we used IVM to study the structure of channel pore and ATP binding site.

3. Experimental questions

The aim of the present study was to contribute to the understanding of the relationship between the molecular structure and function of the rat purinergic $P2X_4$ receptor using its specific modulator – ivermectin. Single point mutagenesis and electrophysiological patch clamp recordings were employed to examine residues involved in activation and deactivation kinetics and ATP sensitivity of $P2X_4$ receptor expressed in HEK cells.

Specifically, the aims of our experiments were to:

1. Identify receptor-specific residues which participate in selective action of ivermectin at $P2X_4$ receptor.

2. Determine the importance of transmembrane residues for the channel function and for the action of ivermectin at $P2X_4$ receptor using the cysteine scanning mutagenesis.

3. Compare the role of several ectodomain residues, which were previously proposed to be important for ATP binding and function of the receptor, by the use of positive allosteric effect of ivermectin.

4. Methods

Cell culture maintenance and transfection

HEK293 cells were grown in Dulbecco′s modified Eagle's medium (DMEM) (Invitrogen, Carlsbad, CA, USA) supplemented with 10% fetal bovine serum, 50 U/ml penicillin and 50 μg/ml streptomycin in a humidified 5% CO_2 atmosphere at 37°C. The day before transfection, the cells were plated on poly-L-lysine coated cover slips in a 35 mm culture dishes at density ~150,000 cells/dish. Transient transfection of the cells was carried out using either wild-type or mutant cDNA (1 μg) and Lipofectamine 2000 (7 μl) in 2 ml of serum-free OptiMEM according to manufacturer's procedure (Invitrogen, Carlsbad, CA, USA). After 4-6 hr of incubation, the transfection mixture was replaced with normal culture medium. The experiments were performed 24 - 48 hr after transfection.

Construction of chimeric and mutant receptors

Chimeric receptors used in this study were constructed by overlap extension PCR method using the corresponding wild-type cDNA as templates in the laboratory of Dr. S.S. Stojilkovic, NICHD, NIH, Bethesda, USA. Chimeras $P2X_{2a}$/V64-Y315$P2X_4$, $P2X_{2b}$/V64-Y315$P2X_4$ contained the V64–Y315 extracellular domain sequence of $P2X_4$ receptor instead of the native I66–Y310 sequence of $P2X_{2a}$ or $P2X_{2b}$ receptor. Reversed chimera contained I66-Y310 sequence of $P2X_2$ instead of V64–Y315 extracellular domain of $P2X_4$ receptor (He, Zemkova et al. 2003). In the chimeric receptor $P2X_{2a}$/V49-V61 $P2X_4$ native I50-E63 sequence of $P2X_2$ receptor was replaced with V49-V61 sequence of the $P2X_4$ receptor and in the $P2X_4$/I50-E63$P2X_{2a}$ chimera native V49-V61 sequence of the $P2X_4$ receptor was replaced with I50-E63 sequence of $P2X_2$ receptor (Jelinkova, Yan et al. 2006).

Point mutant $P2X_4$ receptors were constructed by PCR amplification using the *PfuUltra* high-fidelity DNA polymerase (Stratagene, La Jolla, CA, USA) and specific overlapping oligonucleotide primers (VBC-genomics, Vienna, Austria) and $P2X_4$ receptor cDNA, subcloned in vector pIRES2-EGFP, as a template.

Amplification was carried out according to manufacturer's instructions. Template DNA was digested by *DpnI* (New England Biolabs, Beverely, MA, USA) and PCR mixture was then used for transformation of competent cells *E.coli* JM109 (Promega, Madison, WI, USA). Selected clones were innoculated in LB medium and grown cultures were used for isolation and purification of the plasmid DNA using the Jetquick plasmid spin kit. Each mutation was confirmed by automated DNA sequencing (ABI Prism 3100 Genetic Analyzer, Applied Biosystems, Foster City, CA, USA) in the Laboratory of DNA sequencing, Institute of Microbiology AS CR, vvi.

Patch clamp recordings

Currents were recorded in a whole-cell configuration from HEK293 cells clamped to -60 mV using Axopatch 200B patch-clamp amplifier (Axon Instruments, Union City, CA, USA). Transfected cells were identified by the EGFP fluorescence signal using the Olympus IX71 inverted microscope with fluorescence illuminators (Model IX71; Olympus, Melville, NY, USA). All currents were captured and stored using Digidata 1200A and pClamp8 software package (Axon Instruments, Union City, USA). Patch electrodes were pulled from a glass tube with a 1.65 mm outer diameter on horizontal puller (model P-97, Sutter Instruments, Novato, CA, USA). The tip of the pipette was heat-polished using and its resistance after filling with intracellular solution was 3-5 MΩ. Whole-cell recording was performed using 40% series resistance compensation. During the experiments, the dishes with cell cultures were continuously perfused with an extracellular solution of the following composition (in mM): 142 NaCl, 3 KCl, 2 $CaCl_2$, 1 $MgCl_2$, 10 HEPES and 10 D-glucose, adjust to pH 7.3 with 1 M NaOH. The osmolarity of solution was 290 – 300 mOsm as determined using a vapor pressure osmometer (Model VAPRO 5520; Wescor, Logan, UT). Intracellular solution used for filling of patch electrodes was either K^+ based (composition: 70 mM KCl, 70 mM K-aspartate, 5 mM EGTA, 0.5 mM $CaCl_2$, 1 mM $MgCl_2$, 10 mM HEPES, pH adjusted with 1 M KOH to 7.2), or Cs^+ based (containing 154 mM CsCl, 11 mM EGTA and 10 mM HEPES, pH was adjusted with 1 M CsOH to 7.2). The osmolarity of both solutions was

280-290 mOsm. IVM was dissolved in DMSO to concentration 0.01 M and stored for no more than one week at 4ºC. Prior to experiments it was diluted to required concentrations in extracellular solution. Solutions were applied with a fast gravity driven perfusion system consisting of an array of ten glass tubes terminating into one collective tube of approximately 320 μm in diameter. The end of this collective tube was positioned ~ 500 μm away from the patch pipette and just above the cell culture in an angle ~ 45°. Movement of the glass tube array and solution application was controlled by a step motor and miniature teflon solenoid valves (Parker Hannifinin Corporation, General Valve division, Fairfield, NJ, USA) operated by a microcomputer (Ing. I. Dittert, CSc. and RNDr. V. Vlachova, CSc., Institute of Physiology, AS CR, vvi). A complete change of the solution around a cell took less than 300 ms. Experiments were carried out at room temperature.

Data analysis

Data analysis was carried out using program Clampfit v8, which is included in software pClamp v8 (Axon Instruments, Union City, CA, USA), and using the program Sigmaplot 2000 v6.1 (SPSS Inc., Chicago, IL, USA). To estimate the EC_{50} values, ATP (mostly 0,3-100 μM) was repeatedly applied at 20-120 s intervals and responses were related to the 3 μM ATP response and/or to the maximum current induced by 100 μM ATP (in some cases by 5 mM). This was done to eliminate the influence of $P2X_4$ receptor internalization and slow recovery from desensitization induced by high ATP concentrations (Jones, Chessell et al. 2000). Dose-response data points were fitted by a three-parameter logistic equation using a nonlinear curve-fitting program that derives the EC_{50} values of the produced curves and Hill coefficient (n_H) ($I = 1/(1+(EC_{50}/[ATP])^{n_H}$; I – amplitude of current induced by tested concentration of ATP, EC_{50} – ATP concentration producing 50% of the maximal current response) (SigmaPlot 2000 v6.1; SPSS Inc., Chicago, IL). In some experiments, the EC_{50} values were estimated by extrapolation. The kinetics of current decay evoked by washout of agonists were fitted by a single exponential function ($y = A \exp(t/\tau)+C$, C=0) or by the sum of two exponentials ($y = A_1 \exp(t/\tau_1)$

+ A_2 exp(t/τ_2)+C, C=0) using the program Clampfit v8 (Axon Instruments, Union City, CA, USA). A_1 and A_2 represent current amplitudes, τ_1 and τ_2 time constants, C constant. All numerical values in the text are reported as mean ± SEM, and significant differences, with $P< 0.01$ and 0.05, were determined by Student's *t*- test.

Confocal microscopy

24-48 hours after transient transfection (with wild-type or mutant $P2X_4$ receptor tagged with GFP), HEK293 cells on poly-L-lysine cover slips were washed twice in PBS and then fixed with solution of 2% paraformaldehyd in PBS (pH 7.4) for 15 min on ice. Afterwards, the cells were washed again twice in PBS and left for other 5 min on ice. Then the cells were dehydrated by successive washing in alcohol solutions of different concentration for 1 min (70%, 80% a 95% ethanol). After this washing, cells were mounted in Vectashield medium onto glass slides. The localization of EGFP-tagged receptors was analyzed by using laser scanning confocal microscopy (Leica SP2 AOBS, Leica Microsystems, Wetzlar, Germany). The pictures were collected using the 63x objective lens with applying further zoom (applied wave-length 488 nm).

Helical wheel projection and 3D modeling

Helical wheel projections of TM domains were created using the internet-based application at http://cti.itc.virginia.edu/~cmg/Demo/wheel/wheelApp.html.

5. Results

Identification of $P2X_4$ domains and receptor-specific residues contributing to the ivermectin effects on channel deactivation

Ivermectin (IVM) positively modulates ATP-induced currents in $P2X_4$ receptor. In the presence of IVM (3 μM), the amplitude of current was enlarged for low micromolar ATP concentration up to 20-times and for maximal concentration (100 μM) about 2-times. This potentiating effect was accompanied with an increase in sensitivity of receptor for ATP (EC_{50} value decreased from 6.3 ± 0.6 μM to 0.6 ± 0.3 μM). IVM exhibited also profound effect on channel deactivation (Fig. 1). The time constant of channel deactivation (τ_{off}) increased in the presence of 3 μM IVM from 0.4 ± 0.1 s to 29 ± 3.5 s. Both effects of IVM on $P2X_4$ receptor were time dependent (Jelinkova, Yan et al. 2006; Zemkova, Yan et al. 2007).

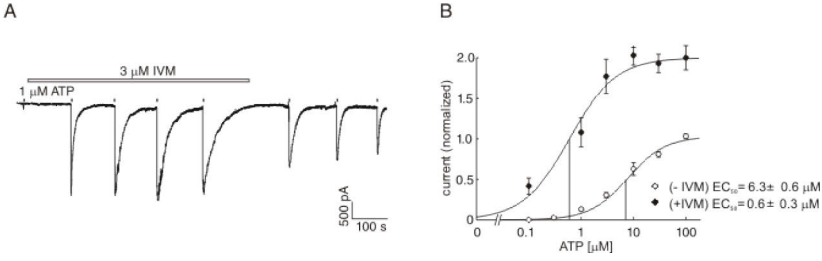

Fig.1 Positive modulatory effect of IVM on ATP-induced current in HEK293 cells expressing $P2X_4$ receptor.

A An example record showing the effect of IVM on the peak amplitude and deactivation time of current induced by repetitive stimulation with 1 μM ATP.

B Concentration dependence of ATP on the peak amplitude of current responses by wild-type (WT) $P2X_4$ receptor in the absence of IVM (open symbols) and in the presence of 3 μM ATP (closed symbols). The vertical lines represent the mean EC_{50} values. Data are presented as mean ± SEM from 5-17 cells.

IVM is effective only when applied extracellularly. To examine the importance of extracellular domain of $P2X_4$ receptor for the IVM effect we used several chimeric receptors of $P2X_4$ and $P2X_2$ receptors (which are IVM insensitive) (Fig. 2).

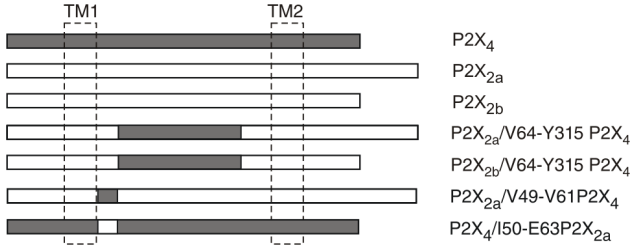

Fig.2 Schematic representation of the wild type and chimeric receptors used in this study. $P2X_{2a}$ and $P2X_{2b}$ are two different splice forms of $P2X_2$ receptor. Dashed boxes represent transmembrane domains.

Chimeric receptors $P2X_{2a}$/V64-Y315$P2X_4$ and $P2X_{2b}$/V64-Y315$P2X_4$ were insensitive to IVM (Jelinkova, Yan et al. 2006) demonstrating that ectodomain sequence V64-Y315 of $P2X_4$ receptor could not transfer the IVM sensitivity to $P2X_2$ receptor. However, the whole ectodomain sequence stretches from W50-I337, consequently two short sequences above the transmembrane domains V49-E63 and G316-I337 had to be tested. Since G316-I337 sequence does not contain any $P2X_4$ receptor-specific residues we tested further the importance of V49-V63 using the pair of chimeric receptors $P2X_{2a}$/V49-V61$P2X_4$ and $P2X_4$/I50-E63$P2X_{2a}$. Both receptors were functional but less sensitive to ATP than WT $P2X_4$ receptor. Chimera $P2X_{2a}$/V49-V61$P2X_4$ was insensitive to IVM. Chimera $P2X_4$/I50-E63$P2X_{2a}$ was sensitive to IVM but only the potentiating effect of IVM was fully preserved. The IVM effect on channel deactivation was dramatically reduced ($\tau_{off} = 1.9 \pm 0.4$ s) compared to WT $P2X_4$ receptor ($\tau_{off} = 29.0 \pm 3.5$ s). These results indicate that the V49-V61 sequence of $P2X_4$ receptor could be important for IVM effect on channel deactivation (Fig. 3).

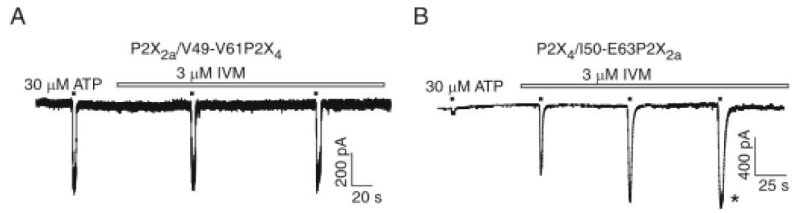

Fig.3 Characterization of the IVM effects on chimeric receptors $P2X_{2a}$/V49-V61$P2X_4$ and $P2X_4$/I50-E63$P2X_{2a}$.

Representative traces of responses to short applications of 30 μM ATP in the absence and in the presence of 3 μM IVM demonstrating the importance of V49-V61 sequence of $P2X_4$ receptor for IVM action.

To examine the potential role of $P2X_4$ receptor-specific residues in V49-V61 sequence (V61, V60, S59, T57 and W50), we substituted these residues by alanine and tested mutated receptors in the presence and absence of IVM. We examined also the $P2X_4$ receptor-specific residues in the first and second transmembrane domain (TM1 and TM2) - M31, A41, V355 and V357 (Fig. 4). All receptors were functional and their sensitivity resembled the sensitivity of WT $P2X_4$ receptor. Mutants $P2X_4$V60A and $P2X_4$V355A exhibited lower current amplitudes which were 54% and 33% of the value measured for WT $P2X_4$ receptor, respectively. In the presence of 3 μM IVM, maximum current amplitudes of all mutant receptors increased 1.7-2.5 fold and also the prolongation of channel deactivation resembled the WT $P2X_4$ receptor with the exception of 3 receptors: $P2X_4$W50A (τ_{off} = 5.9 ± 1.8 s) and $P2X_4$V357A (τ_{off} = 10.1 ± 2.3 s) receptors exhibited reduced deactivation effect of IVM compared to WT $P2X_4$ receptor, while $P2X_4$V60A exhibited enhanced deactivation effect (τ_{off} = 46.6 ± 5.4 s).

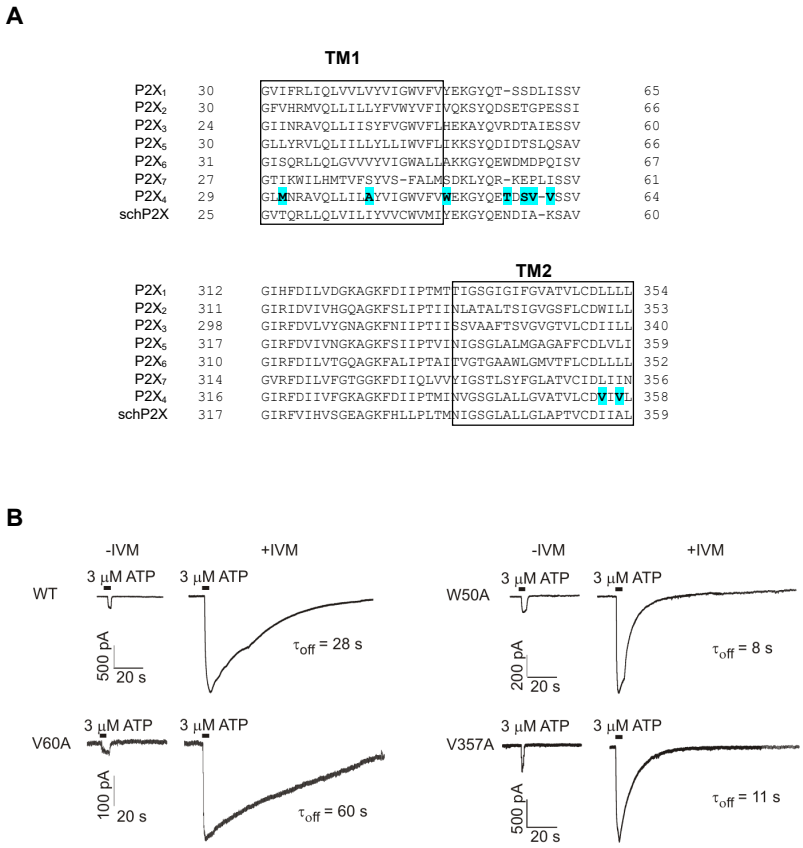

Fig. 4 Characterization of $P2X_4$ receptor-specific mutant receptors.

A Sequence alignment of transmembrane domains and adjacent parts of extracellular domains (which were not included in $P2X_{2a}$/V64-Y315$P2X_4$ and $P2X_{2b}$/V64-Y315$P2X_4$ chimeric receptors) of rat P2X receptors and P2X receptor from *Schistosoma mansoni* (schP2X), which is also IVM sensitive. Blue colour marks the $P2X_4$ receptor-specific residues.

B Representative recording of responses to short applications of 3 μM ATP in the absence and in the presence of 3 μM IVM demonstrating the differences in the rate of deactivation.

These results suggest the potential importance of receptor-specific residues W50, V60 and V357 for the effect of IVM on $P2X_4$ receptor.

Identification of the transmembrane residues responsible for the effect of IVM on $P2X_4$ receptor

The results with chimeric receptors and $P2X_4$ receptor-specific mutants indicated that the effect of IVM is independent of ectodomain structure and cannot be abolished by the substitution of receptor-specific residues. Moreover, the results have shown that also both transmembrane domains could be important for IVM action. Therefore we studied the importance of all transmembrane residues for the effect of IVM on $P2X_4$ receptor. Both transmembrane domains are suggested to play a key role in channel activation, especially gating, consequently this study was also done to elucidate the importance of these residues for the receptor function.

We performed cysteine scanning mutagenesis of residues in both TM1 (G29-W50) and TM2 (N338-L358) and tested the function of mutant receptors in the presence and absence of 3 μM IVM. All TM1 mutant receptors were functional. However, $P2X_4$G29C, $P2X_4$R33C, $P2X_4$Y42C, $P2X_4$W46C and $P2X_4$V49C receptors exhibited significantly lower current amplitudes compared to WT $P2X_4$ receptor. For the $P2X_4$G29C and $P2X_4$V49C receptors we could not determine their EC_{50} values. Mutants $P2X_4$M31C and $P2X_4$R33C displayed lower sensitivity to ATP contrary to $P2X_4$Y42C and $P2X_4$G45C mutants that showed higher sensitivity to ATP. In the case of $P2X_4$Y42C receptor, we observed also changes in channel deactivation which was largely prolonged. We assume that residues substituted in mutants with significant changes in EC_{50}, I_{max} and τ_{off} could play an important role in the receptor function. For other TM1 mutant receptors ($P2X_4$L30C, $P2X_4$N32C, $P2X_4$A34C, $P2X_4$V35C, $P2X_4$Q36C, $P2X_4$L37C, $P2X_4$L38C, $P2X_4$I39C, $P2X_4$L40C, $P2X_4$A41C, $P2X_4$V43C, $P2X_4$I44C, $P2X_4$V47C, $P2X_4$F48C and $P2X_4$W50C) we did not observe significant changes in EC_{50} and I_{max} (Tab. 1). Therefore these residues were suggested to be tolerant to cysteine substitution.

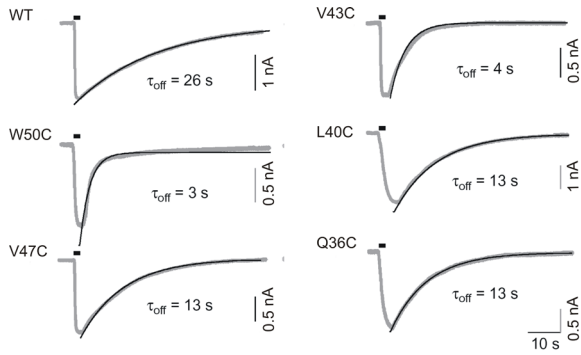

Fig.5 Characterization of mutagenesis-tolerant TM1 mutants.
Representative recordings of responses to short applications exhibiting changes in IVM deactivation effect to 1-3 μM ATP in the presence of 3 μM IVM. All these receptors were mutagenesis-tolerant but they exhibited reduced deactivation time constant (τ_{off}) in the presence of IVM compared to WT receptor. Grey traces represent the experimental records, black lines show the fitted curves derived using monoexponential fitting.

In the presence of IVM, majority of mutagenesis tolerant residues showed increase in I_{max}, prolongation of channel deactivation and reduced EC_{50} comparable to WT $P2X_4$ receptor. However, there were some exceptions. In the case of $P2X_4Q36C$, $P2X_4L40C$, $P2X_4V43C$, $P2X_4V47C$ and $P2X_4W50C$ receptors we observed reduced IVM effect on deactivation and ATP sensitivity compared to WT $P2X_4$ receptor (Fig. 5, Tab. 1). Since these receptors were mutagenesis-tolerant we suggest that these changes reflect the importance of corresponding residues for recognition of IVM molecule.

In the presence of IVM, we also observed differences in the function of mutagenesis-sensitive receptors. In case of these receptors, the interpretation of the results was more complicated because the changes in IVM effect could reflect not only the reduction of receptor function but also the changes in IVM binding. Firstly we looked whether the changes in the rate of IVM-induced deactivation of these receptors could be explained by changes in ATP sensitivity since both these

parameters are inversely related and should change in parallel (Li, Migita et al. 2004). We also examined whether the fold increase of EC_{50} and I_{max} is comparable to WT $P2X_4$ receptor (fold increase of EC_{50} = 65, fold increase of I_{max} = 1.75).

The function of $P2X_4$G29C and $P2X_4$V49C receptors, which were almost nonfunctional in the absence of IVM, was rescued in the presence of IVM; however, the sensitivity remained decreased compared to WT $P2X_4$ receptor. The decreased sensitivity was accompanied with enhanced rate of channel deactivation, indicating that predicted correlation of both parameters was present. Based on these observations we suggest that V49 residue is important for channel function and not for IVM binding. The explanation of results obtained for $P2X_4$G29C receptor was similar; however, in the case alanine mutant (data not presented in this work) decreased ATP sensitivity in the presence of IVM was not accompanied with a change in the rate of channel deactivation. Therefore we assume that G29 is important not only for channel function but also for the IVM binding. Changes of time deactivation constant in other substitution-sensitive receptors $P2X_4$M31C and $P2X_4$G45C were also parallel to changes in their sensitivity to ATP, therefore we suggest that they do not participate in the recognition of IVM molecule. Another mutation-sensitive receptor $P2X_4$R33C displayed also the rightward shift in the sensitivity to ATP but that was not accompanied with the proportional increase in the deactivation. Therefore we suggest that differences in channel behavior we observed in the presence of IVM were induced not only by the changes in the receptor function but also by the impairment of the recognition of the IVM molecule. $P2X_4$Y42C receptor was very specific since we did not observe any increase in I_{max} and sensitivity in the presence of IVM and the rate of receptor deactivation was enhanced already in the absence of IVM. We observed similar decay of current also in the presence of ATP (τ_{des} = 41.2 ± 5.2 s). Therefore we suggest that this decrease reflects also the desensitization of the receptor. Finally, the $P2X_4$W46C also displayed reduced I_{max} though the sensitivity and deactivation was comparable to WT $P2X_4$ receptor (Tab. 1). However, this receptor responded to ATP stimulation with lower current amplitudes even in the absence of IVM and the fold increase of current amplitude was comparable to WT $P2X_4$ receptor. We assume that in this case

reduced amplitude could result from a lower expression of the receptor in the membrane.

Tab.1 IVM effects on WT and TM1-mutant $P2X_4$ receptors.

$P2X_4$ receptor	-IVM EC_{50} (μM)	+IVM EC_{50} (μM)	-IVM I_{max} (nA)	+IVM I_{max} (nA)	-IVM τ_{off} (s)	+IVM τ_{off} (s)
WT	4.6±0.3	0.5±0.1	1.6±0.2	2.8±0.2	0.4±0.04	26±1.6
W50C	7.3±1.9	2.2±0.1*	1.6±0.4	2.5±0.3	0.5±0.20	4±0.4*
V49C#	n.d.	1.8±0.3*	0.3±0.1*	0.9±0.3*	0.4±0.05	15±1.9*
F48C	3.8±1.3	0.5±0.2	1.2±0.3	1.9±0.3	0.4±0.1	31±2.8
V47C	3.6±1.2	1±0.1	1.3±0.2	2±0.1*	0.3±0.01	16±1.6*
W46C	6.2±0.2	0.4±0.1	1±0.2*	1.4±0.3*	0.5±0.16	26±2.7
G45C	1.6±0.3*	0.2±0.03	1.8±0.3	2.9±0.5	0.4±0.04	76±9.3*
I44C	4.1±0.4	0.4±0.03	2.1±0.5	2.6±0.3	0.3±0.03	31±4.6
V43C	4.5±0.5	2.2±0.4*	1.4±0.4	2.2±0.5	0.3±0.15	2.7±0.5*
Y42C	0.6±0.1*	0.5±0.1	0.5±0.2*	0.4±0.2*	21±1.8*	32±4.2
A41C	5.1±0.8	0.7± 0.4	1.6±0.3	2.4±0.2	0.3±0.05	26±2.9
L40C	7.2±1.2	1.7±0.5*	1.2±0.1	2.7±0.2	0.2±0.09	13±1.3*
I39C	4.6±1.3	0.5±0.1	1.3±0.3	2.1±0.4	0.2±0.18	30±3.6
L38C	7.4±2.5	0.9±0.1	1.8±0.2	2.4± 0.4	0.2±0.03	19±2.1
L37C	6.3±0.7	0.9±0.2	1.8±0.9	2.3±0.2	0.3±0.05	22±2.5
Q36C	7.4±2.5	1.9±0.2*	1.4±0.2	2.5±0.4	0.2±0.03	13±2.0*
V35C	4.1±1.0	0.6±0.3	1.5±0.2	2±0.5	0.3±0.04	37±3.2
A34C	3.9±1.1	0.5±0.5	2.0±0.4	2.5±0.4	0.3±0.05	24±2.1
R33C	9.9±1.8*	2.9±1.4*	0.6±0.1*	0.8±0.2*	0.7±0.2	22±2.8
N32C	6±0.9	0.8±0.1	2±0.3	2.8±0.4	0.4±0.07	20±4.7
M31C#	15±2*	1±0.2	1.1±0.2	2.6±0.3	0.3±0.15	17±2.5*
L30C	5.7±0.7	0.9±0.2	1.3±0.3	2.6±0.4	0.3±0.02	21±3.0
G29C#	n.d.	4.9±0.7*	0.1±0.05*	0.5±0.1*	0.3±0.02	16±1.3*

EC_{50} - ATP concentration producing 50% of the maximal current response; I_{max} - maximum amplitude of current induced by 30-100 μM ATP (# determined with the concentration 1 mM ATP), τ_{off} - deactivation time constant of currents after removal of ATP; n.d. - not determined. Each receptor was examined in the presence (+IVM) or absence (-IVM) of 3μM IVM. (*) – significant differences ($P<0.01$) between WT and mutated receptor.

We substituted with cysteine also all residues from TM2 (N338-L358). All mutant receptors were functional with the exception of $P2X_4$D354C. Using confocal microscopy, we proved the localization of this receptor in the membrane indicating that ATP binding or gating was affected by this substitution. $P2X_4$S341C, $P2X_4$G347C, $P2X_4$T350C and $P2X_4$V357C receptors exhibited significantly reduced I_{max} compared to WT $P2X_4$ receptor but their sensitivity to ATP remained

unaffected. In the case of $P2X_4C353A$ receptor, the decrease in I_{max} was accompanied by a significant increase in EC_{50} and $P2X_4L343C$ receptor showed highly reduced sensitivity to ATP. The $P2X_4G340C$ receptor was the only TM2 mutant that showed reduced EC_{50}. It showed also prolonged deactivation in the absence of IVM and thus resembled the TM1 mutants $P2X_4Y42C$. Mutant $P2X_4A344C$ was exceptional as it exhibited progressive run-down of current during repetitive stimulations with ATP. The other TM2 mutant receptors were tolerant to cysteine mutagenesis (Tab. 2).

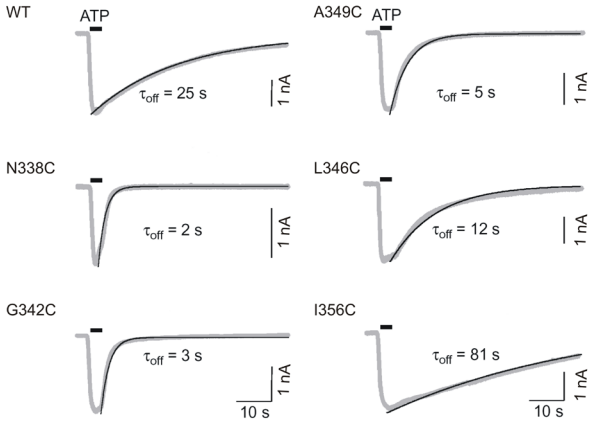

Fig.6 Characterization of cysteine substitution-tolerant mutant receptors from TM2 exhibiting changes in IVM-induced deactivation effect.

Representative recordings of responses to short applications to 1-3 μM ATP in the presence of 3 μM IVM. All these receptors exhibited altered rate of deactivation in the presence of IVM compared to WT receptor. Grey traces represent the records, black lines show the fitted curves derived using monoexponential fitting.

In the presence of IVM, some mutant receptors (both tolerant and sensitive to mutagenesis) displayed changes in behavior compared to WT $P2X_4$ receptor. The decay of current of $P2X_4N338C$, $P2X_4G342C$, $P2X_4L346C$ and $P2X_4A349C$ receptors was faster than the decay of WT $P2X_4$ receptor. Changes in the rate of

deactivation were parallel to changes in their sensitivity to ATP induced by IVM. $P2X_4$I356C receptor deactivated more slowly than WT $P2X_4$ receptor (Fig. 6, Tab. 2). All these receptors were tolerant to cysteine substitution, therefore we assume that the observed differences in their behavior were caused only by affected binding of the IVM molecule.

For the evaluation of changes in IVM effects on TM2 substitution-sensitive receptors we used the same approach as we employed for the results with TM1 mutant receptors. $P2X_4$C353A receptor exhibited in the presence of IVM reduced sensitivity to ATP but the rate of deactivation remained unchanged. Therefore we suggest that this residue is important for both – channel function and IVM binding. Mutants $P2X_4$S341C, $P2X_4$G347C, $P2X_4$T350C and $P2X_4$V357C, that showed reduced current responses in the absence of IVM, responded to ATP stimulation with lower current amplitudes also in the presence of IVM. Their sensitivity and deactivation were comparable to WT $P2X_4$ receptor with the exception of $P2X_4$S341C.The fact that IVM-induced fold increase of I_{max} in $P2X_4$T350C $P2X_4$G347C and $P2X_4$V357C receptors was comparable or even higher than in WT $P2X_4$ receptor suggests that this residues are not critical for IVM binding. Receptor $P2X_4$S341C showed increase in the current decay together with the decrease in sensitivity to ATP (Tab. 2); currently we have no explanation for this effect.

Tab.2 IVM effects on WT and TM2 cysteine mutant $P2X_4$ receptors.

$P2X_4$ receptor	-IVM EC_{50} (μM)	+IVM EC_{50} (μM)	-IVM I_{max} (nA)	+IVM I_{max} (nA)	-IVM τ_{off} (s)	+IVM τ_{off} (s)
WT	4.6±0.3	0.5±0.1	1.6±0.2	2.8±0.2	0.4±0.1	26±1.6
N338C	4.6±0.8	2.5±1.1*	1±0.3	2.4±0.3	0.5±0.1	1.9±0.1*
V339C	3.8±0.2	0.7±0.1	2.3±0.4	3.4±0.5	0.6±0.1	27±0.4
G340C	0.7±0.1*	0.6±0.2	0.8±0.2*	0.9±0.2 *	3.8±0.3*	15±1.5*
S341C[#]	6±1.1	1.8±0.5*	0.5±0.1*	1.3±0.2*	0.6±0.1	12±1.4*
G342C	3.1±0.5	2.2±0.5*	1.4±0.2	2.8±0.3	1.7±0.2*	3.8±0.5*
L343C[#]	>100	15±2.6*	1.6±0.3	2.7±0.3	0.7±0.1	4.2±0.5*
A344C	3.4±0.5	n.d.	1.3±0.3	n.d.	0.7±0.1	26±3.7
L345C	6.5±1.7	1±0.4	1.8±0.5	2.8±0.4	0.9±0.3	19±2.1
L346C	3.3±0.7	2.1±0.5*	1.5±0.3	2.7±0.4	0.8±0.2	4.3±1.2*
G347C	7.5±0.4	0.8±0.2	0.5±0.1*	2.4±0.4	0.6±0.1	20±2.9
V348C	3.2±0.6	0.7±0.2	1.7±0.5	3±0.3	0.7±0.1	22±1.8
A349C	4.5±0.5	1.4±0.4*	1.1±0.3	2.3±0.4	0.4±0.1	10±1.5*
T350C	4.8±1	0.7±0.5	0.9±0.2*	1.8±0.3*	0.7±0.1	34±3.3
V351C	5.1±0.7	1.3±0.2*	1.4±0.3	2.7±0.4	0.5±0.04	19±1.9
L352C	5.5±1.2	0.7±0.1	1.1±0.2	2.3±0.2	0.4±0.1	20±3.1
C353A	10±3.2*	2.3±1.1*	0.7±0.1*	1.3±0.4*	0.2±0.05	24±2.5
D354C	-	-	-	-	-	-
V355C	4.7±1.5	0.7±0.2	1.2±0.5	1.8±0.2*	0.4±0.04	21±2.2
I356C	4.4±1.2	0.8±0.1	1.2±0.5	2.2±0.4	0.3±0.03	51±7.1*
V357C	3.2±1.3	0.5±0.3	0.6±0.1*	1.5±0.2*	0.4±0.07	34±1.4
L358C	2.5±1.6	0.6±0.2	1.2±0.1	1.7±0.2*	0.3±0.07	30±2.2

EC_{50} - ATP concentration producing 50% of the maximal current response; I_{max} - maximum amplitude of current induced by 30-100 μM ATP ([#] determined with the concentration 1 mM ATP), τ_{off} - deactivation time constant of currents after removal of ATP; n.d. - not determined. Each receptor was examined in the presence (+IVM) or absence (-IVM) of 3μM IVM. (*) – significant differences ($P<0.01$) between WT and mutated receptor.

The pattern of IVM-induced changes of receptor function at substitution-tolerant receptors is consistent with α-helical topology of both TM domains. Therefore we plotted the TM1 sequence (G29-V49), together with W50, and TM2 sequence (N338-L358) onto helical wheel projections (Fig.7). Residues which were substitution-tolerant (Q36, L40, V43, V47 and W50) but displayed weaken effects of IVM map specifically to one side of predicted helix. Similarly N338, G342, L346, A349 and I356 residues, which were tolerant to mutagenesis and displayed altered effect of IVM, lie on the same side of TM2 α-helix. On the opposite side to

substitution tolerant residues with IVM hits, there are residues sensitive to substitution (with the exception of S341) in both helices.

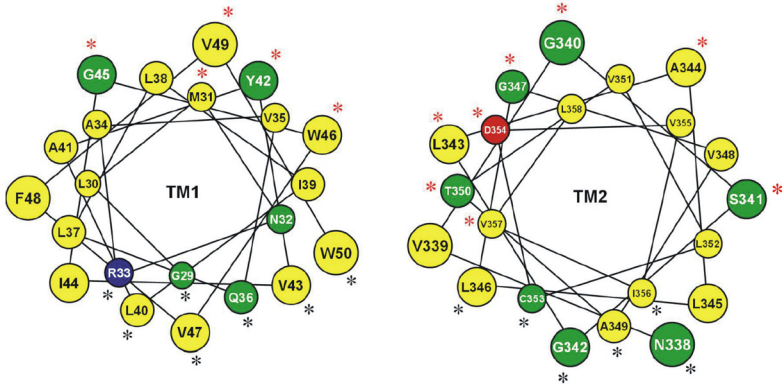

Fig.7 Helical wheel projection of TM1 and TM2 domains of $P2X_4$ receptor.

The plots show predicted α-helical structure of the TM1 segment (G29-W50) and TM2 segment (N338-L358) viewed from the extracellular side of the membrane. (*) indicates cysteine substitution-tolerant residues that exhibited changes in IVM effects on τ_{off}s, together with G29, R33 and C535 which probably also participate on IVM binding. (*) labels residues which were sensitive to substitution and this substitution did not influence the IVM binding. Colours indicate nonpolar (yellow), polar uncharged (green), basic (blue) and acidic (red) residues.

The evaluation of the role of aromatic and charged residues for $P2X_4$ function with the use of positive modulatory effect of IVM

In this study we also focused on ectodomain residues which had been proposed to participate in binding of ATP and/or channel gating at the P2X receptor: K67, K69, F185, K190, F230, R278, D280, N293, R295, R308 and K313 ($P2X_4$ numbering). We created alanine and rescue mutant receptors and tested their function. As a control we choose other three residues in the extracellular domain (K197, K258 and N287) and substituted them with alanine.

All random mutants, P2X$_4$K197A, P2X$_4$K258A and P2X$_4$N287A, were functional and their sensitivity and deactivation resembled WT P2X$_4$ receptor both in the absence and presence of IVM (3.8±0.3 μM and 0.5±0.1 μM) (Tab. 3).

Mutants P2X$_4$K67A and P2X$_4$K67R stimulated with 1 mM ATP responded with current amplitude that was only about 6% of that observed in WT P2X$_4$ receptor, though their perimembrane expression was at comparable levels as expression of WT P2X$_4$ receptor (Zemkova, Yan et al. 2007). Therefore we could not determine their EC$_{50}$. However, in the presence of IVM, we observed several-fold potentiation of current amplitudes and increase in ATP sensitivity (Fig. 8, Tab. 3). The estimated EC$_{50}$ values were in a milimolar range. These results indicate that both receptors were functional but had dramatically decreased sensitivity to ATP. The absence of difference between these two receptors indicates that arginine could not substitute lysine at this position.

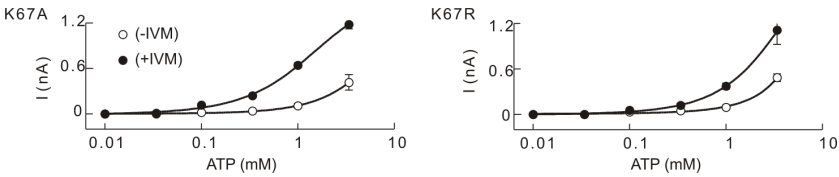

Fig.8 Characterization of P2X$_4$K67A and P2X$_4$K67R mutant receptors.
Concentration dependence of ATP on the peak amplitude of current responses by P2X$_4$K67A (left) and P2X$_4$K67R (right) receptors in the absence of IVM (open symbols) and in the presence of 5 μM IVM (closed symbols). Data are presented as mean ± SEM from 5-18 cells.

Also P2X$_4$K190A and P2X$_4$R278A mutants responded to 1 mM ATP with low current amplitudes (13% and 31% of WT P2X$_4$ receptor) and their EC$_{50}$ could not be determined. In the presence of IVM, these receptors were fully functional (Fig. 9) and their EC$_{50}$ values were only 40- and 4-fold increased as compared with WT P2X$_4$ receptor. Contrary to alanine mutants, the rescued P2X$_4$K190R and P2X$_4$R278K receptors were functional even in the absence of IVM. These data indicate that positive charge is important at these positions.

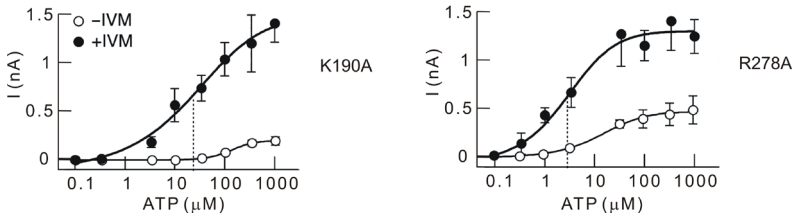

Fig.9 Characterization of $P2X_4K190A$ and $P2X_4R278A$ mutant receptors.
Concentration dependence of ATP on the peak amplitude of current responses by $P2X_4K190A$ (left) and $P2X_4R278A$ (right) receptors in the absence of IVM (open symbols) and in the presence of 5 μM IVM (closed symbols). Data are presented as mean ± SEM from 4-13 cells. Dashed vertical lines represent EC_{50} values estimated in the presence of IVM.

The function of $P2X_4R295A$ and $P2X_4K313A$ receptors was severely damaged and introduction of the positive charge ($P2X_4R295K$ and $P2X_4K313R$) did not rescue the receptor function. Therefore we could not determine the EC_{50} values of these receptors. All receptors were expressed in the perimembrane region at levels comparable to WT $P2X_4$ receptor (Yan, Liang et al. 2005; Zemkova, Yan et al. 2007) and were functional in the presence of IVM although EC_{50} values were several fold increased (57 μM to 420 μM) when compared to WT $P2X_4$ receptor. In the presence of IVM, we observed only slight difference between alanine and rescue mutants (Tab. 3).

The $P2X_4F230A$ receptor responded only to submilimolar or milimolar concentrations of ATP contrary to $P2X_4F230W$ receptor which was fully functional. In the presence of IVM, also $P2X_4F230A$ receptor was functional with EC_{50} of about 1 μM. However, we observed highly reduced current amplitude compared to WT $P2X_4$ receptor (12 - 18% of WT $P2X_4$ receptor) (Tab. 3). The confocal images proved lower expression of this receptor in the membrane and its retention in endoplasmaticum reticullum (Zemkova, Yan et al. 2007).

Also the EC_{50} value of $P2X_4F185A$ receptor could not be determined since this receptor responded only to submilimolar or milimolar concentration of ATP. But confocal microscopy proved its perimembrane localization (Zemkova, Yan et al. 2007). In the presence of IVM, the receptor was fully functional with EC_{50} of 4 μM. The function of $P2X_4F185W$ receptor was similar to that of WT $P2X_4$ receptor which indicates importance of aromatic residue in this position. In the case of $P2X_4F294A$ receptor, we did not observed significant difference from WT $P2X_4$ receptor in the presence of IVM (Fig. 10, Tab. 3).

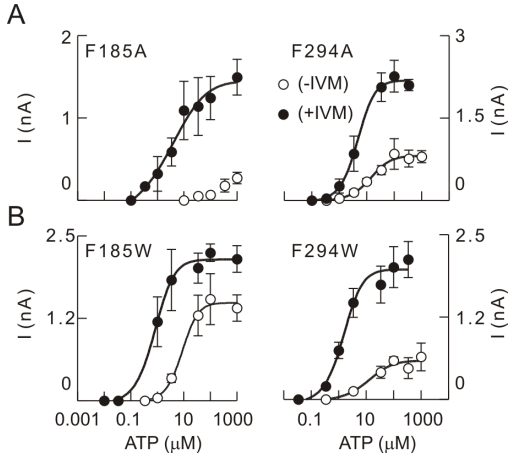

Fig.10 Characterization of $P2X_4F185A$/ $P2X_4F185W$ and $P2X_4F294A$/ $P2X_4F294W$ mutant receptors.

A Concentration dependence of ATP on the peak amplitude of current responses by $P2X_4F185A$ (left) and $P2X_4F294A$ (right) receptors in the absence of IVM (open symbols) and in the presence of 5 μM IVM (closed symbols).

B Concentration dependence of ATP on the peak amplitude of current responses by $P2X_4F185W$ (left) and $P2X_4F294W$ (right) receptors in the absence of IVM (open symbols) and in the presence of 5 μM IVM (closed symbols). Data are presented as mean ± SEM from 3-15 cells.

Next we examined deactivation properties of all ectodomain mutants. With the exception of $P2X_4$F185A, $P2X_4$F185W and $P2X_4$R278K receptors, the deactivation of all mutant receptors was significantly reduced in the presence of IVM compared to WT $P2X_4$ receptor. Receptors $P2X_4$K67A/$P2X_4$K67R, $P2X_4$R295A/$P2X_4$R295K and $P2X_4$K313A/$P2X_4$K313R showed the most enhanced rate of deactivation and we did not observe significant differences in deactivation kinetics for these pairs of mutants (Tab. 3). Therefore we suggest that these residues are important for receptor structure or function and that their role is not given only by the charge of molecule. On the other hand, the $P2X_4$K190A/$P2X_4$K190R and $P2X_4$R278A/$P2X_4$R278K pairs of mutants exhibited huge differences in deactivation (Tab. 3): alanine mutants deactivated much faster than rescue mutants. The differences in deactivation of these pairs of mutants were parallel to differences in EC_{50} values. Therefore we suggest that positive charge of these residues (K190 and R278) is important at these positions. The deactivation of $P2X_4$F230A, $P2X_4$F230W, $P2X_4$F294A and $P2X_4$F294W mutants was also accelerated. However, the effect of substitution of these aromatic residues was not so dramatic as it was with lysine or arginine residues. We observed that there was a correlation between EC_{50} and τ_{off} (R= -0.68). This fact suggests that the potency of agonist contributes to control of receptor function.

Tab.3 Characterization of WT and ectodomain mutant $P2X_4$ receptors.

Receptor	-IVM EC_{50} (μM)	+IVM EC_{50} (μM)	-IVM I_{max} (nA)	+IVM I_{max} (nA)	+IVM τ_{off} (s)
WT $P2X_4$	3.8±0.3	0.5±0.1	1.6±0.1	2.9±0.2	24.5±1.0
K197A	5.7±1.3	0.9±0.2	0.6±0.2*	1.5±0.3*	19.5±1.3
K258A	3.1±1.8	0.2±0.1	1.7±0.3	2.8±0.4	22.8±4.9
N287A	5.3±0.7	0.7±0.3	0.6±0.1*	1.3±0.2 *	20.1±2.3
K67A	n.d.	997±105^	0.1±0.03*	0.5±0.1*	2.5±0.3 *
K67R	n.d.	2293±450^	0.1±0.03*	0.4±0.1*	3.6±0.4*
F185A	n.d.	3.7±1.5*	0.3±0.09*	1.9±0.3	18.9±1.2
F185W	7±1.5	1±0.2	1.5±0.4	2.2±0.2	21.8±3.7
K190A	n.d.	18.9±1.2*	0.2±0.02*	1.4±0.3*	4.5±0.6*
K190R	10.7±2.4	2.1±0.2*	0.7±0.04	1.2±0.1*	18.5±1.3*
F230A	n.d.	1±0.2	0.2±0.05*	0.5±0.2*	8.7±0.9*
F230W	4.6±1.7	1.4±0.4	1.5±0.3	2.5±0.85	15.6±1.7*
R278A	n.d.	1.9±0.4*	0.5±0.15*	1.4±0.3*	7.8±0.8*
R278K	3±0.9	0.9±0.2	0.9±0.15*	1.6±0.2	38.6±6.3*
D280A	n.d.	0.9±0.3	0.5±0.03*	1.5±0.2*	6.9±1.1*
D280E	3.2±1.2	0.5±0.2	1.1±0.5	2.0±0.2	11.1±2.4*
F294A	31.4±5*	3.2±0.8*	0.8±0.11*	1.9±0.3	10.9±1.4*
F294W	13.6±2.2*	1.3±0.4	0.6±0.06*	2.1±0.3	17.6±1.7*
R295A	n.d.	267±41*	0.5±0.07*	2.2±0.3	5.3±0.5*
R295K	n.d.	57±12*	0.6±0.17*	2.1±0.2	6.2±0.6*
K313A	n.d.	420±80*	0.2±0.04*	1.3±0.2	3.3±0.3*
K313R	n.d.	125±56*	0.4±0.08*	1.8±0.2	4.6±0.4*

EC_{50} - ATP concentration producing 50% of the maximal current response; I_{max} - maximum amplitude of current induced by 1 mM ATP (^ - determined by extrapolation), τ_{off} - deactivation time constant of currents after removal of ATP; n.d. - not determined. Each receptor was examined in the presence (+IVM) or absence (-IVM) of 5 μM IVM. (*) – significant differences ($P<0.01$) between WT and mutant receptor.

6. Conclusions

1. We found that bulky ectodomain of $P2X_4$ receptor, sequence V64-Y315, does not participate in IVM specific effect on $P2X_4$ receptor. Contrary to this, both transmembrane domains and the sequence V49-V61 above the TM1 play an important role in IVM action.

2. Alanine substitution of any of $P2X_4$ receptor-specific residues studied does not abolish the potentiation induced by IVM. In the case of $P2X_4$W50A, $P2X_4$V60A and $P2X_4$V357A mutant receptors we observed changes in the rate of IVM-induced deactivation.

3. Amino acid residues in both transmembrane domains (Q36, L40, V43, V47, N338, G342, L346, A349 and I356) together with W50, which were tolerant to cysteine mutagenesis, are oriented to lipid bilayer in an open state and probably form a binding pocket for IVM molecule.

4. We confirmed helical conformation of both TM domains. We identified residues in TM1 and TM2 (M31, Y42, G45, W46, V49, G340, S341, L343, A344, G347, T350, D354 and V357) that are oriented into the hydrophilic channel pore and play important role in receptor function.

5. We demonstrated that several ectodomain mutants, previously reported as nonfunctional, were in functional in the presence of IVM.

6. Using IVM, we made an order of ectodomain residues potentially involved in ATP binding and identified K67, R295 and K313 as the most important for $P2X_4$ receptor function.

7. References

Agboh KC, Webb TE, Evans RJ and Ennion SJ (2004) Functional characterization of a P2X receptor from Schistosoma mansoni. *J Biol Chem* **279**(40):41650-41657.

Barrera NP, Ormond SJ, Henderson RM, Murrell-Lagnado RD and Edwardson JM (2005) Atomic force microscopy imaging demonstrates that P2X2 receptors are trimers but that P2X6 receptor subunits do not oligomerize. *J Biol Chem* **280**(11):10759-10765.

Brake AJ, Wagenbach MJ and Julius D (1994) New structural motif for ligand-gated ion channels defined by an ionotropic ATP receptor. *Nature* **371**(6497):519-523.

Edwards G (2003) Ivermectin: does P-glycoprotein play a role in neurotoxicity? *Filaria J* **2 Suppl 1**:S8.

Egan TM, Haines WR and Voigt MM (1998) A domain contributing to the ion channel of ATP-gated P2X2 receptors identified by the substituted cysteine accessibility method. *J Neurosci* **18**(7):2350-2359.

Ennion S, Hagan S and Evans RJ (2000) The role of positively charged amino acids in ATP recognition by human P2X1 receptors. *J Biol Chem* **275**(45):35656.

Freist W, Verhey JF, Stuhmer W and Gauss DH (1998) ATP binding site of P2X channel proteins: structural similarities with class II aminoacyl-tRNA synthetases. *FEBS Lett* **434**(1-2):61-65.

Gever JR, Cockayne DA, Dillon MP, Burnstock G and Ford AP (2006) Pharmacology of P2X channels. *Pflugers Arch* **452**(5):513-537.

Haines WR, Migita K, Cox JA, Egan TM and Voigt MM (2001) The first transmembrane domain of the P2X receptor subunit participates in the agonist-induced gating of the channel. *J Biol Chem* **276**(35):32793-32798.

He ML, Zemkova H and Stojilkovic SS (2003) Dependence of purinergic P2X receptor activity on ectodomain structure. *J Biol Chem* **278**(12):10182-10188.

Jelinkova I, Yan Z, Liang Z, Moonat S, Teisinger J, Stojilkovic SS and Zemkova H (2006) Identification of P2X4 receptor-specific residues contributing to the ivermectin effects on channel deactivation. *Biochem Biophys Res Commun* **349**(2):619-625.

Jiang LH, Rassendren F, Spelta V, Surprenant A and North RA (2001) Amino acid residues involved in gating identified in the first membrane-spanning domain of the rat P2X(2) receptor. *J Biol Chem* **276**(18):14902-14908.

Jones CA, Chessell IP, Simon J, Barnard EA, Miller KJ, Michel AD and Humphrey PP (2000) Functional characterization of the P2X(4) receptor orthologues. *Br J Pharmacol* **129**(2):388-394.

Khakh BS and Egan TM (2005) Contribution of transmembrane regions to ATP-gated P2X2 channel permeability dynamics. *J Biol Chem* **280**(7):6118-6129.

Khakh BS, Proctor WR, Dunwiddie TV, Labarca C and Lester HA (1999) Allosteric control of gating and kinetics at P2X(4) receptor channels. *J Neurosci* **19**(17):7289-7299.

Li Z, Migita K, Samways DS, Voigt MM and Egan TM (2004) Gain and loss of channel function by alanine substitutions in the transmembrane segments of the rat ATP-gated P2X2 receptor. *J Neurosci* **24**(33):7378-7386.

Migita K, Haines WR, Voigt MM and Egan TM (2001) Polar residues of the second transmembrane domain influence cation permeability of the ATP-gated P2X(2) receptor. *J Biol Chem* **276**(33):30934-30941.

Newbolt A, Stoop R, Virginio C, Surprenant A, North RA, Buell G and Rassendren F (1998) Membrane topology of an ATP-gated ion channel (P2X receptor). *J Biol Chem* **273**(24):15177-15182.

Nicke A, Baumert HG, Rettinger J, Eichele A, Lambrecht G, Mutschler E and Schmalzing G (1998) P2X1 and P2X3 receptors form stable trimers: a novel structural motif of ligand-gated ion channels. *Embo J* **17**(11):3016-3028.

Priel A and Silberberg SD (2004) Mechanism of ivermectin facilitation of human P2X4 receptor channels. *J Gen Physiol* **123**(3):281-293.

Rassendren F, Buell G, Newbolt A, North RA and Surprenant A (1997) Identification of amino acid residues contributing to the pore of a P2X receptor. *Embo J* **16**(12):3446-3454.

Roberts JA and Evans RJ (2004) ATP binding at human P2X1 receptors. Contribution of aromatic and basic amino acids revealed using mutagenesis and partial agonists. *J Biol Chem* **279**(10):9043-9055.

Roberts JA and Evans RJ (2006) Contribution of conserved polar glutamine, asparagine and threonine residues and glycosylation to agonist action at human P2X1 receptors for ATP. *J Neurochem* **96**(3):843-852.

Roberts JA, Vial C, Digby HR, Agboh KC, Wen H, Atterbury-Thomas A and Evans RJ (2006) Molecular properties of P2X receptors. *Pflugers Arch* **452**(5):486-500.

Silberberg SD, Chang TH and Swartz KJ (2005) Secondary structure and gating rearrangements of transmembrane segments in rat P2X4 receptor channels. *J Gen Physiol* **125**(4):347-359.

Torres GE, Egan TM and Voigt MM (1998) Topological analysis of the ATP-gated ionotropic [correction of ionotrophic] P2X2 receptor subunit. *FEBS Lett* **425**(1):19-23.

Valera S, Hussy N, Evans RJ, Adami N, North RA, Surprenant A and Buell G (1994) A new class of ligand-gated ion channel defined by P2x receptor for extracellular ATP. *Nature* **371**(6497):516-519.

Vial C, Roberts JA and Evans RJ (2004) Molecular properties of ATP-gated P2X receptor ion channels. *Trends Pharmacol Sci* **25**(9):487-493.

Yan Z, Liang Z, Tomic M, Obsil T and Stojilkovic SS (2005) Molecular determinants of the agonist binding domain of a P2X receptor channel. *Mol Pharmacol* **67**(4):1078-1088.

Zemkova H, Yan Z, Liang Z, Jelinkova I, Tomic M and Stojilkovic SS (2007) Role of aromatic and charged ectodomain residues in the P2X(4) receptor functions. *J Neurochem* **102**(4):1139-1150.

8. List of publications

Zemkova H., Yan Z., Liang Z., Jelinkova I., Tomic M. and Stojilkovic S.S. (2007) Role of aromatic and charged ectodomain residues in the P2X(4) receptor functions. *J Neurochem.* **102**(4): 1139-1150.

Jelinkova I., Yan Z., Liang Z., Moonat S., Teisinger J., Stojilkovic S.S. and Zemkova H. (2006) Identification of $P2X_4$ receptor specific residues contributing to the ivermectin effects on channel deactivation. *Biochem. Biophys. Res. Commun.* **349**(2): 619 – 625.

Mazna P., Berka K., Jelinkova I., Balik A., Svoboda P., Obsilova V., Obsil T. and Teisinger J. (2005) Ligand binding to the human MT2 melatonin receptor: The role of residues in transmembrane domains 3, 6 and 7. *Biochem. Biophys. Res. Commun.* **332**(3): 726-734.

Mazna P., Obsilova V., Jelinkova I., Balik A., Berka K., Sovova Z., Rudiger E., Svoboda P., Obsil T. and Teisinger J. (2004) Molecular modeling of human MT2 melatonin receptor: the role of Val 204, Leu 272 and Tyr 298 in ligand binding. *J. Neurochem.* **91**(6): 836-842.